AMERICAN SOCIETY FOR MICROBIOLOGY | Journal of Virology®

VIRUS-CELL INTERACTIONS

MC159 of Molluscum Contagiosum Virus Suppresses Autophagy by Recruiting Cellular SH3BP4 via an SH3 Domain-Mediated Interaction

Constanze Schmotz,[a] Hasan Uğurlu,[a] Silja Vilen,[a] Subhash Shrestha,[a] Riku Fagerlund,[a] Kalle Saksela[a]

[a]Department of Virology, University of Helsinki, Helsinki University Hospital, Helsinki, Finland

ABSTRACT MC159 is a viral FLIP (FLICE inhibitory protein) encoded by the molluscum contagiosum virus (MCV) enabling MCV to evade antiviral immunity and to establish persistent infections in humans. Here, we show that MC159 contains a functional SH3 binding motif, which mediates avid and selective binding to SH3BP4, a signaling protein known to regulate endocytic trafficking and suppress cellular autophagy. The capacity to bind SH3BP4 was dispensable for regulation of NF-κB-mediated transcription and suppression of proapoptotic caspase activation but contributed to inhibition of amino acid starvation-induced autophagy by MC159. These results provide new insights into the cellular functions of MC159 and reveal SH3BP4 as a novel host cell factor targeted by a viral immune evasion protein.

IMPORTANCE After the eradication of smallpox, molluscum contagiosum virus (MCV) is the only poxvirus restricted to infecting humans. MCV infection is common and causes benign skin lesions that usually resolve spontaneously but may persist for years and grow large, especially in immunocompromised individuals. While not life threatening, MCV infections pose a significant global health burden. No vaccine or specific anti-MCV therapy is available. MCV encodes several proteins that enable it to evade antiviral immunity, a notable example of which is the MC159 protein. In this study, we describe a novel mechanism of action for MC159 involving hijacking of a host cell protein called SH3BP4 to suppress autophagy, a cellular recycling mechanism important for antiviral immunity. This study contributes to our understanding of the host cell interactions of MCV and the molecular function of MC159.

KEYWORDS MC159, MVC, SH3 domain, SH3BP4, autophagy, protein-protein interactions, vFLIP

Molluscum contagiosum virus (MCV) belongs to the *Poxviridae* family and is the sole known member of the *Molluscipox* genus (1, 2). It is the only poxvirus that can cause a persistent infection in humans, and since the eradication of smallpox, it is the only poxvirus with a host range restricted to humans. Although not life threatening, MCV infections pose a significant global health burden. MCV causes a common and typically benign skin disease with characteristic small lesions known as mollusca, which usually resolve spontaneously in weeks to months but may persist for years (1, 2). However, in immunocompromised individuals much larger lesions and a more severe course of the disease can be seen. To date no direct treatment for MCV infection exists.

Molluscum lesions show few or no signs of inflammation (3, 4), presumably reflecting the battery of immunoevasion factors encoded by the MCV genome (5, 6). One prominent factor is MC159, which together with MC160 of MCV and similar proteins of gammaherpesviruses (such as Kaposi's sarcoma-associated herpesvirus [KSHV]), constitutes a protein family known as viral FLIPs ([vFLIPs] FLICE inhibitory proteins; FLICE stands for FADD-like interleukin-1beta-converting enzyme and is better known as

Citation Schmotz C, Uğurlu H, Vilen S, Shrestha S, Fagerlund R, Saksela K. 2019. MC159 of molluscum contagiosum virus suppresses autophagy by recruiting cellular SH3BP4 via an SH3 domain-mediated interaction. J Virol 93:e01613-18. https://doi.org/10.1128/JVI.01613-18.

Editor Joanna L. Shisler, University of Illinois at Urbana Champaign

Address correspondence to Kalle Saksela, kalle.saksela@helsinki.fi.

Received 12 September 2018
Accepted 20 February 2019
Accepted manuscript posted online 6 March 2019
Published 1 May 2019

procaspase-8) (7–9). Cellular homologues of vFLIPs (splice isoforms $cFLIP_L$, $cFLIP_S$, and $cFLIP_R$) also exist and serve as key apoptotic regulators of the cell (10, 11).

All FLIPs consist of two death effector domains (DED) that they use to interact with FADD and procaspase-8, but the antiapoptotic potency and detailed mechanisms of action of different FLIPs deviate substantially (for a review, see reference 12). MC159 was recently shown to inhibit caspase-8 filament assembly via a unique capping mechanism (13). The antiapoptotic function of MC159 has also been reported to involve TRAF3 binding sites in the C-terminal region that is unique to MC159 (14). Unlike the vFLIP of KSHV whose antiapoptotic function depends on its potent capacity to activate NF-κB-driven gene expression (15, 16), MC159 mediates only a weak increase or no increase in basal cellular NF-κB activity. Instead, MC159 efficiently inhibits NF-κB induced by stimuli, such as tumor necrosis factor receptor (TNFR) engagement, thereby blunting the proinflammatory aspects of NF-κB function (for a review, see reference 12). The mechanistic basis of NF-κB inhibition by MC159 has recently been elucidated and shown to involve targeting of the IKK complex to prevent cellular inhibitor of apoptosis protein 1 (cIAP1)-induced polyubiquitination of NEMO (17, 18).

In addition to inhibiting the activation of procaspase-8 and NF-κB, MC159 may also contribute to MCV immunoevasion via further mechanisms. Randall and colleagues found that MC159 can suppress interferon gene activation by inhibiting TANK-binding kinase 1 (TBK1)-mediated activation of the interferon regulatory factor 3 (IRF3) transcription factor by a mechanism that is distinct from its inhibitory targeting of NF-κB (19). Furthermore, MC159 as well as other cellular and viral FLIPs have been shown to suppress cellular autophagy (20). This may be important for persistence of MCV infection because autophagy constitutes a prominent cellular defense system that can suppress viral replication by multiple mechanisms, including promotion of virus recognition by intracellular innate sensors (21–23).

A common strategy utilized by viruses to promote their replication and to interfere with antiviral immunity is to hijack host cell signal transduction pathways by incorporating into their proteomes functional binding motifs for modular protein interaction domains (PID), such as the Src-homology region-3 (SH3) domain (reviewed in reference 24). SH3 domains represent the most ubiquitous class of PID (≈300 encoded by the human genome) and mediate a plethora of important protein interactions that regulate normal and pathological cell behavior (25). SH3 domains are composed of a beta-barrel fold of approximately 60 amino acid residues, which bind to short proline-containing target peptides but can also acquire additional binding affinity and specificity via more complex contacts with their ligand proteins (26).

Since the discovery and characterization of the interaction between the HIV-1 pathogenicity factor Nef with the tyrosine kinase Hck (27–29), we have described several other examples of SH3-mediated host cell interactions involving viral proteins such as NS5A of hepatitis C virus, NS1 of influenza A virus, and nsP3 of chikungunya and other alphaviruses (30–33). To facilitate these efforts, we have developed a screening platform based on an essentially complete collection of human SH3 domains assembled into a phage display library that allows unbiased affinity-based screening of preferred SH3 partners for potential SH3 ligands as native full-length proteins (34, 35). In this study, we have used this discovery platform to identify human SH3 domain-binding protein 4 (SH3BP4) as a novel interaction partner for MC159 and characterized the role of this interaction in modulating cellular functions of MC159.

RESULTS

Identification of MC159 as an SH3 domain ligand. To identify novel viral ligands for cellular SH3 domains, we scanned sequences of viral proteins from the Swiss-Prot/TrEMBL database using the ScanProsite search engine. This revealed the MC159 protein from MCV as a potential candidate containing two short sequences corresponding to consensus SH3 binding motifs (26), one at the N terminus partly overlapping the first

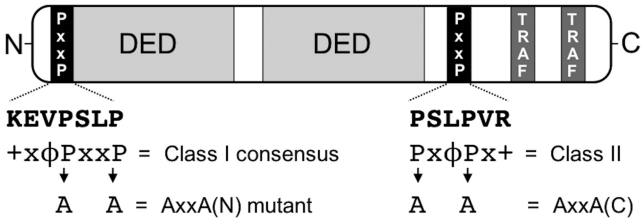

FIG 1 Structural organization of MC159. Shown are the relative positions of the tandem death effector domains (DED), the C-terminal TRAF-binding motifs, and the proline-rich (PXXP) motifs in the 241-amino-acid MC159 polypeptide. The sequences of the PXXP motifs are shown and aligned with class I and class II consensus SH3 domain binding motifs. The alanine substitution strategy for disrupting these motifs to create MC159 mutants AXXA(N) and AXXA(C) is also indicated.

DED and another between the second DED and the tandem TRAF binding sites in the C-terminal region of MC159 (Fig. 1).

To examine the SH3 binding capacity and potential SH3 partner specificity of MC159, we expressed it in human 293T cells fused to a biotin acceptor domain (BD) and bound it to streptavidin-coated beads for affinity screening of a phage display library composed of a virtually complete ($n = 296$) human SH3 phage display library (34). In contrast to control beads coated with BD only, beads coated with MC159 showed a robust (>20-fold) enrichment of phages after a single round of affinity selection, indicating MC159 as an avid SH3 ligand (Fig. 2). When the identities of the SH3 domains of MC159-selected phage clones were determined by DNA sequencing, the SH3 domain of SH3 binding protein 4 (SH3BP4) (36) (also known as TTP [37]) was found to be highly dominant, representing 80 to 100% of the sequenced clones in several independent phage library screens (Fig. 2). No other individual SH3 domains were significantly and reproducibly enriched in these experiments. Thus, our library screen identified SH3BP4 as a robust and highly preferred SH3 domain partner of MC159.

To investigate the role of the two SH3 consensus target sequences (PXXP motifs) of MC159 in SH3BP4 SH3 binding, we generated MC159 mutants having either one or both of these motifs disrupted by a double-alanine substitution (PXXP to AXXA) (Fig. 1) and tested these mutants as affinity ligands for SH3 phage display library screening. Disruption of the C-terminal proline motif [MC159$^{AXXA(C)}$] had no effect on the strong

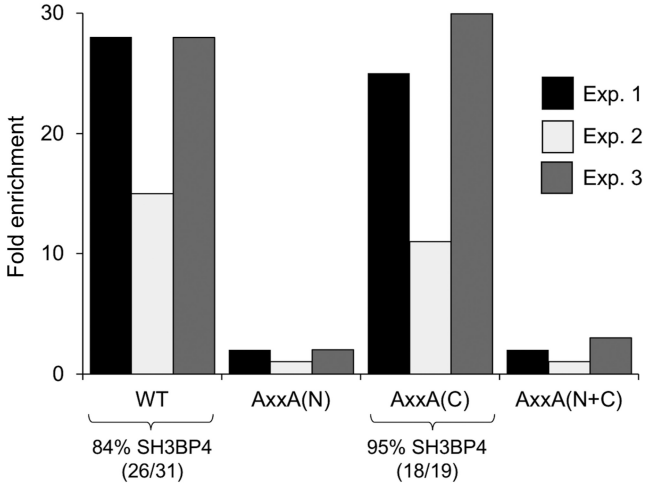

FIG 2 Phage display library screening for host cell SH3 protein partners of MC159. The relative increase in the captured SH3-displaying phages in three independent experiments (Exp. 1 to 3) using the wild type (WT) and the indicated mutants of MC159 protein as affinity baits compared to levels using beads coated with control protein is indicated as fold enrichment. The proportions of SH3BP4 SH3-containing clones among the phage genomes sequenced from the enriched phage populations selected by wild-type MC159 and MC159$^{AXXA(C)}$ are shown below the bar diagram.

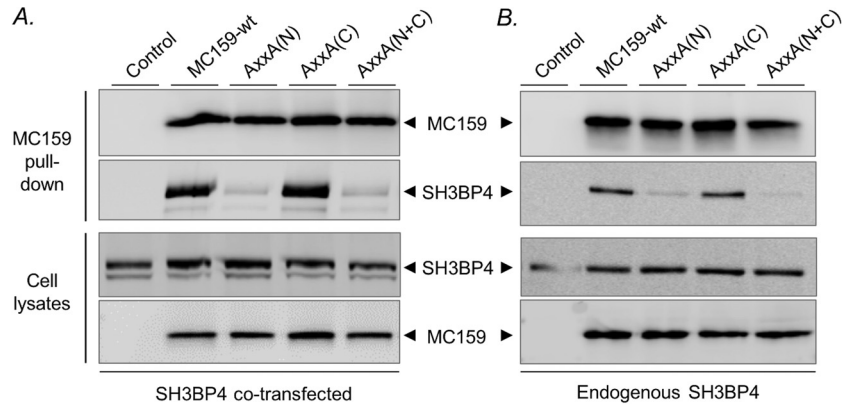

FIG 3 Association of MC159 with SH3BP4 in human cells. Biotin acceptor domain-tagged MC159 or the indicated PXXP motif mutants were transfected into 293T cells together with Myc-tagged SH3BP4 (A) or SH3BP4 alone (B). Lysates of these cells were examined by Western blotting either directly (cell lysates) or after precipitation with streptavidin-coated beads (MC159 pulldown) by probing the membranes using labeled streptavidin (MC159) or anti-Myc (A) or anti-SH3BP4 (B) antibodies.

capacity of MC159 for SH3 phage enrichment (Fig. 2). In contrast, mutation of the N-terminal motif alone [MC159$^{AXXA(N)}$] or in combination with the C-terminal motif [MC159$^{AXXA(N+C)}$] efficiently abrogated SH3 binding, resulting in a failure to enrich phages compared to levels with a mock control (Fig. 2). Thus, we concluded that the N-terminal class I SH3 consensus motif (KEVPSLP) in MC159 mediated its avid binding to the SH3 domain of SH3BP4, whereas, despite the resemblance to a class II consensus sequence, the C-terminal PXXP motif of MC159 showed no evidence of serving as a functional SH3 binding site.

In an attempt to reveal additional SH3 domains with weaker affinity toward MC159 whose binding might have been masked by the robust binding of SH3BP4 SH3, we performed further phage library screens with a library from which SH3BP4 SH3 had been excluded. However, no additional SH3 domains with specific affinity for MC159 could be identified, suggesting that among the human SH3 repertoire, SH3BP4 is unique in its selectivity for avid MC159 binding.

Association of full-length SH3BP4 with MC159 in cells. To examine binding of native full-length SH3BP4 to MC159 in human cells we cotransfected 293T cells with vectors encoding these proteins appended to Myc and BD tags. Western blotting of proteins coprecipitating with MC159 captured with streptavidin-coated beads revealed an intense anti-Myc blotting signal for detecting SH3BP4, whereas no SH3BP4 was found to coprecipitate with negative-control beads (Fig. 3A).

In agreement with the phage display results, mutation of the N-terminal PXXP motif of MC159 efficiently disrupted SH3BP4 association, whereas mutation of the C-terminal PXXP motif did not affect SH3BP4 coprecipitation. A faint residual SH3BP4 signal was still associated with the MC159$^{AXXA(N)}$ protein but not with mock-pulldown protein, suggesting that additional weak contacts between MC159 and SH3BP4 might also take place. However, since this weak residual association was shared also by MC159$^{AXXA(N+C)}$, a role for the C-terminal PXXP motif in contributing to this interaction could be excluded.

MC159 binding was not restricted to overexpression of SH3BP4 as coprecipitation of endogenous SH3BP4 with MC159 could also be readily demonstrated in 293T cells transfected with MC159 alone (Fig. 2B). Also, the observed effects of the PXXP-disrupting mutations in MC159 were the same when binding to endogenous instead of overexpressed and Myc-tagged SH3BP4 was studied (Fig. 3B).

Impact of SH3BP4 binding capacity on cellular functions of MC159. Blunting of the activation of proapoptotic caspases and activation of NF-κB-mediated transcription triggered by stimulation of the death receptors Fas and TNFR1 are well studied cellular effects of MC159 and thought to be important for its role as an MCV immune evasion

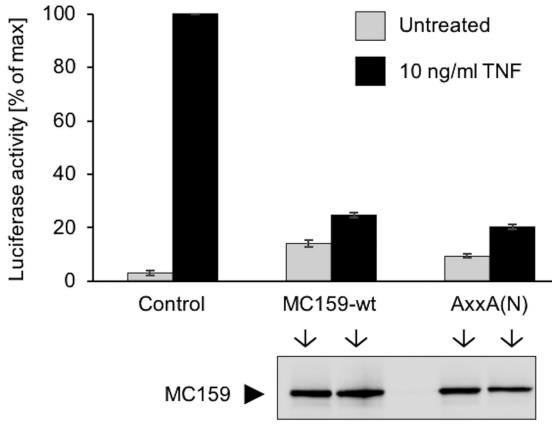

FIG 4 Regulation of NF-κB activity by MC159 and its SH3BP4 binding-deficient mutant. Luciferase activity was measured in lysates of 293T cells transfected with an NF-κB-driven reporter plasmid alone (Control) or with WT MC159 or MC159$^{AXXA(N)}$ with no treatment or after 8 h of stimulation with 10 ng/ml TNF. Uniform expression of MC159 in the cotransfected cells was confirmed by Western blotting (bottom panel).

factor (12). We therefore examined the impact of the SH3 binding capacity of MC159 to these functions.

In agreement with previous data (18, 38, 39), we found that transient transfection of wild-type (WT) MC159 into 293T cells together with a luciferase reporter vector resulted in a modest increase in the basal NF-κB activity but efficiently suppressed potent NF-κB activation induced by TNF treatment of these cells (Fig. 4). However, abrogation of SH3BP4 binding capacity had little impact in this regard as MC159$^{AXXA(N)}$ showed a very similar capacity to modulate NF-κB activity.

To examine the role of SH3 binding of MC159 in antagonizing caspase-mediated apoptotic cell death, we transfected wild-type MC159 and MC159$^{AXXA(N)}$ into HeLa cells and monitored induction of apoptosis by analyzing proteolytic cleavage of caspase-8 and -3 following TNF treatment combined with cycloheximide-induced sensitization. Caspase cleavage was determined by Western blotting to detect the disappearance of intact caspase-3 and the appearance of caspase-8 cleavage products (Fig. 5). While the previously described (7–9, 40) ability of MC159 to prevent proapoptotic caspase activation was obvious, mutations in the SH3 binding site of MC159 had no effect on this function (Fig. 5). Thus, the loss of SH3BP4 association did not positively or negatively modulate the ability of MC159 to block caspase activation, a function reported to be dependent on the double DED (41) and also attributed to the C-terminal TRAF-binding sites of MC159.

Many virally encoded inhibitors of autophagy have been discovered (21–23), and such a function has also been reported for MC159 (20). Since SH3BP4 has also been independently linked to the autophagic regulation (42, 43), it was of particular interest to examine the capacity of MC159 and its SH3BP4 binding-deficient mutant to regulate cellular autophagy. To this end, we used a lentiviral vector to stably transduce wild-type MC159 and MC159$^{AXXA(N)}$ fused with the red fluorescent protein mCherry into a previously characterized MCF7-derived macroautophagy reporter cell line expressing the LC3 protein fused to enhanced green fluorescent (MCF-7/LC3-EGFP cells) (44).

The two stably transduced cell populations gave similar and strong signals specific for the MC159-mCherry fusion protein in Western blotting and showed similar patterns of red decoration in immunofluorescent microscopy (Fig. 6A to C). The parental MCF-7/LC3-EGFP cells showed low basal levels of cytoplasmic green autophagosome speckles under normal culture conditions (a median of three $>$1-μm-diameter autophagosomes per cell), and their sizes or average numbers per cell did not noticeably differ in cells transduced with wild-type MC159 or MC159$^{AXXA(N)}$ (Fig. 6A).

When the MCF-7/LC3-EGFP cells were placed into a culture medium lacking amino acids and other nutrients, a substantial increase in the number (median, 17) of the

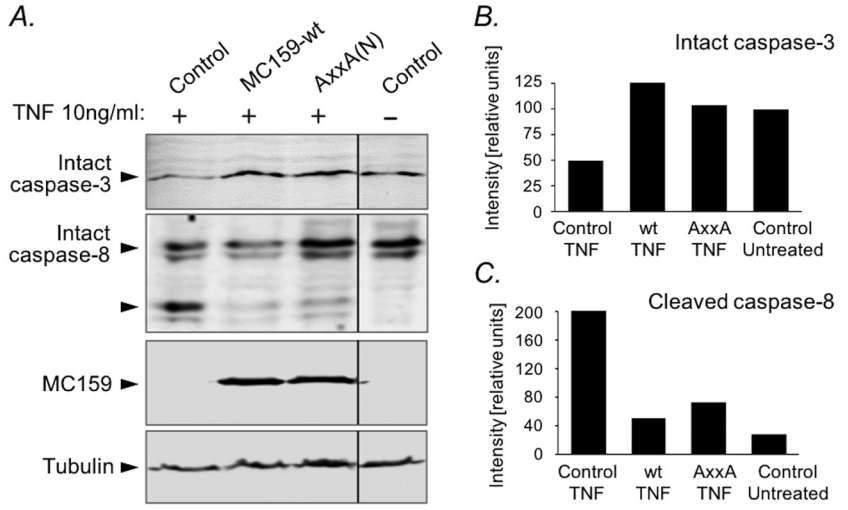

FIG 5 Regulation of proapoptotic caspase activation by MC159 and its SH3BP4 binding-deficient mutant. HeLa cells were transfected with wild-type MC159, MC159$^{AXXA(N)}$, or an empty control vector and later treated for 8 h with 10 ng/ml TNF combined with 10 μg/ml cycloheximide (TNF) or left untreated as indicated. Induction of apoptosis was monitored by Western blotting to detect the cleavage of caspase-3 and -8 (A). Graphs quantifying the detected signals are shown on the right as bar diagrams for caspase-3 that remained intact (B) and for the appearance of cleaved caspase-8 (C). Equal expression levels of MC159 in the transfected cells and uniform loading of cell lysates in the gel were monitored by detection of MC159 and tubulin. Removal of two irrelevant lanes from the blots shown in panel A is marked by vertical black lines.

autophagosomes became evident in 6 h (Fig. 6B), presumably as a consequence of suppression of the amino acid-stimulated Rag GTPase-TORC1 (target of rapamycin complex 1) signaling pathway (45, 46). In agreement with previous data reported by Lee et al. (20), in the cell population stably expressing wild-type MC159, only a modest increase in autophagosomes was observed upon amino acid starvation, and the LC3-EGFP fluorescence pattern in these cells remained more similar to that seen in cells grown in complete culture medium (Fig. 6B). In contrast, the MC159$^{AXXA(N)}$-transduced cell population responded to starvation with an autophagy induction that was as robust as that seen in control cells not expressing any MC159. Equal expression of wild-type and mutant MC159 proteins in the transduced cell populations, as well as equal expression of the LC3-EGFP reporter protein in all three cell populations, was confirmed by Western blotting (Fig. 6C). A summary of the data on automated image analysis of changes in the number of autophagosomes under different conditions in three independent experiments involving a total of 20,181 MCF-7/LC3-EGFP cells examined is shown as a box plot in Fig. 6E.

As an alternative approach for examining autophagic activity independently of LC3 fluorescence or morphological imaging, we examined the starvation-induced disappearance of p62 in these cells. p62 is an adaptor protein for autophagic cargo, which in this process becomes degraded itself, thereby serving as a useful indicator of the autophagic flux (47, 48). Indeed, we noticed a profound (34-fold; i.e., down to 3.7% of untreated) decrease in p62 levels in cells subjected to 6 h of starvation (Fig. 6D). In cells expressing wild-type MC159 the starvation-induced degradation of p62 also occurred but was much less pronounced (12-fold). In contrast, in cells expressing the SH3BP4 binding-deficient MC159$^{AXXA(N)}$ mutant, the loss of p62 was even enhanced compared to expression in the control cells. Thus, these data corroborate the capacity of MC159 to suppress starvation-induced autophagy and further confirm the critical role of the SH3BP4 binding site of MC159 in this process.

To directly prove that the correlation between SH3BP4 binding and autophagy suppression by MC159 was due to functional involvement of SH3BP4, we used CRISPR/Cas9 technology to knock out SH3BP4 from MCF-7/LC3-EGFP cells and generated

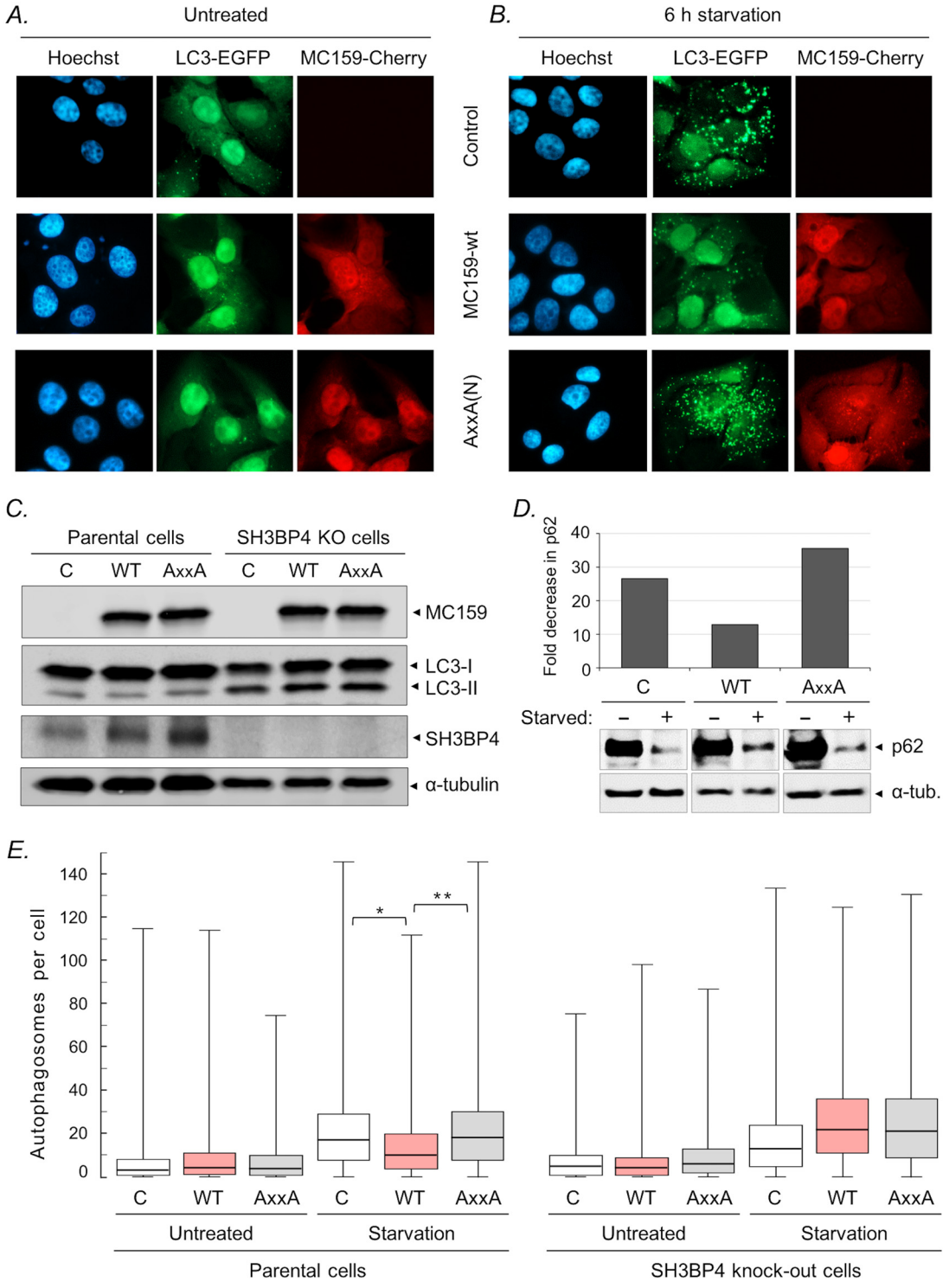

FIG 6 Regulation of autophagy by MC159 and its SH3BP4 binding-deficient mutant. (A and B) Control MCF-7/LC3-EGFP cells or their lentivirally transduced derivatives stably expressing wild-type MC159 or MC159$^{AXXA(N)}$ were examined under normal culture conditions (A) or after 6 h of starvation (B) in medium lacking amino acids and serum using fluorescence microscopy imaging of nuclear (Hoechst)-, LC3-, and MC159-specific signals, as indicated. (C) Uniform LC3-GFP expression in all cells, equal MC159 expression in the transduced cells, and the lack of SH3BP4 expression in the knockout cells were verified by Western blotting using antibodies against GFP, mCherry, and SH3BP4, respectively. (D) Decrease of p62 expression in MCF-7/LC3-EGFP cells (control, C) and their derivatives expressing wild-type MC159 (WT) or MC159$^{AXXA(N)}$ (AXXA) was examined by Western blotting. The anti-p62 signals were quantified and normalized to levels of the corresponding loading control values (anti-α-tubulin signal) to calculate the relative decrease in p62 expression, which is shown as a bar graph above the blot. (E) Box blot presentation of the data from automated quantification of the number of autophagosomes in the parental MCF-7/LC3-EGFP cells and their SH3BP4 knockout derivatives used as controls (C) or transduced with wild-type MC159 (WT) or MC159$^{AXXA(N)}$ (AXXA), as indicated. The boxes mark

(Continued on next page)

lentivirally transduced populations that stably expressed wild-type MC159 or MC159$^{AXXA(N)}$. The lack of SH3BP4 expression and equal expression of MC159 in these cells were confirmed by Western blotting (Fig. 6C). The lack of SH3BP4 had no obvious effect on the basal level of autophagy as measured by counting LC3-GFP-positive autophagosomes (Fig. 6E), but starvation-induced autophagy was slightly attenuated, which is in agreement with the reported role of SH3BP4 as a negative regulator of amino acid-Rag GTPase-mTORC1 signaling (43). In contrast to the parental MCF-7/LC3-EGFP cells, MC159 could no longer counteract starvation-induced autophagy in the SH3BP4 knockout cells, and no difference in the numbers of autophagosomes could be observed between cells expressing wild-type and mutant MC159 (Fig. 6E). Based on these data, we conclude that the ability of MC159 to suppress starvation-induced autophagy is indeed mediated via its binding to the host cell protein SH3BP4.

DISCUSSION

The FLIP family was first recognized as a group of procaspase-8-like proteins encoded by MCV and various gammaherpesviruses (vFLIPs) (7–9), which were soon found to have cellular counterparts (cFLIPs) serving as key regulators of apoptotic cell death (10). Subsequently FLIPs have also been described as inhibitors of autophagy (20). The present study started from the observation that, unlike other cellular or viral FLIPs, the MC159 protein of MCV contained peptide motifs suggestive of SH3 binding. We found that an N-terminal peptide motif was indeed a functional SH3 binding site and among the human SH3 repertoire avidly and selectively recruited the SH3 domain of SH3BP4.

Considering that this sequence looks like an archetypal class I SH3 consensus binding motif, the nearly exclusive specificity of MC159 for binding to SH3BP4 was striking. It is possible that, besides the consensus binding motif, additional noncanonical contacts between MC159 and the SH3 domain of SH3BP4 also contribute to the selectivity of this interaction. Elucidation of the molecular basis of this binding specificity using structural biology approaches could therefore be a worthwhile future endeavor.

Although only a few papers addressing the function of SH3BP4 have so far been published, it has emerged as an interesting protein involved in important cellular processes. SH3BP4 has been shown to regulate the internalization of the transferrin receptor, intriguingly mediated via its apparent capacity to allow cargo-specific control of clathrin endocytosis (37). On the other hand, and relevant to this study, SH3BP4 has been reported to interfere with amino acid-controlled activation of the mammalian target of rapamycin complex 1 (mTORC1), a master regulator of cellular autophagy (43). Specifically, it was shown that binding of SH3BP4 to Rag GTPases prevented their association with mTORC1, resulting in suppression of amino acid-induced mTORC1 activity and, thereby, inhibition of cell growth and promotion of autophagy.

Because previous work has independently also linked MC159 to regulation (inhibition) of autophagy, it was of special interest for us to study the MC159-SH3BP4 interaction in the context of autophagy induction. We found that disruption of the SH3BP4 binding site in MC159 strongly compromised the capacity of MC159 to counteract starvation-induced autophagy. The functional requirement of SH3BP4 in this process was confirmed by knockout experiments showing that, in cells lacking SH3BP4, this binding site became irrelevant and that wild-type MC159 had lost its capacity to suppress starvation-induced autophagy.

Since binding of SH3BP4 to Rag GTPases has been shown to be SH3 dependent (43), a simple scenario whereby MC159 would inhibit autophagy by competing with Rag GTPases for binding to SH3BP4 could, thus, be easily envisaged. However, the mech-

FIG 6 Legend (Continued)
the two middle quartiles of the data points separated by a line showing the median autophagosome count, and the whiskers show the distribution of all values in the upper and lower data point quartiles. The statistical significance of the indicated comparisons is shown as follows: *, $P = 6{,}291 \times 10^{-93}$; **, $P = 5{,}868 \times 10^{-101}$.

anism of action of MC159 might be more complex because of the following: (i) disruption of the SH3 binding site of MC159 strongly diminished but did not completely abrogate its capacity to suppress inhibition of autophagy; (ii) despite lacking SH3BP4-binding sites, other viral and cellular FLIPs can also inhibit autophagy, apparently due to their capacity to prevent Atg3 from binding and processing LC3 (20). Regarding the latter point, however, when we consider the diversity in the molecular mechanisms used by different FLIPs to antagonize apoptosis (12), there is no reason to expect that all FLIPs would share just a single strategy for suppressing autophagy. Nevertheless, studies on the relative contribution or possible cooperation of SH3BP4 and Atg3 binding in the anti-autophagy function of MC159 could be informative. However, addressing this question may not be a straightforward task because mutation of the residues in KSHV vFLIP protein K13 mediating its binding to Atg3 resulted in a more general damage to K13 functionality, including a failure to regulate NF-κB signaling as well as to suppress caspase activation (20). In any case, based on our current data it can be concluded that the occurrence of a functional SH3 binding motif of MC159 enabling the recruitment of SH3BP4 potently contributes to its capacity for autophagy suppression, a feature of MCV evolution that distinguishes MC159 from other FLIPs.

In contrast to suppression of autophagy, other functions of MC159 that we examined were not compromised by the loss of the SH3BP4 interaction. MC159 with a disrupted SH3BP4 binding site showed wild-type-like potency (i) in modestly elevating the basal cellular level of NF-κB activity, (ii) in potently inhibiting strong NF-κB activation induced by TNF stimulation, and (iii) in counteracting proteolytic activation of procaspase-8 and -3 in TNF-treated cells. Thus, the SH3 binding independence of these established MC159 functions indicates that SH3BP4 is specifically involved in mediating the anti-autophagy effect of MC159 rather than being a host cell factor more generally required for supporting MC159 functionality.

While involvement of SH3BP4 in fundamental cellular processes has been reported previously (37, 43), much remains to be learned from its role in cell biology. SH3BP4 has no close relative in the human genome but shares significant homology and a similar domain architecture with metastasis-associated in colon cancer 1 (MACC1), a regulator of hepatocyte growth factor (HGF)/Met signaling with value as a cancer biomarker (49). While this sequence homology does not provide obvious new insights into SH3BP4 function, it is worth noting that recent studies on cancer genetics have also implicated SH3BP4 as an important factor in human cancer pathogenesis. A genome-scale screen of microRNA-related single nucleotide polymorphisms (SNP) carried out by Wilkins et al. revealed an SNP in the 3′ untranslated region of SH3BP4 to be strongly associated with survival of laryngeal cancer (50). On the other hand, SH3BP4 was one of the most significant hits identified by Zhang et al. in a study examining differentially expressed genes associated with metastatic prostate cancer (51). Thus, further studies on SH3BP4, including the role of SH3BP4 in regulation of endocytic trafficking and autophagy, are clearly warranted and, in addition to elucidating the immunoevasion mechanisms enabling MCV to establish a persistent infection, could lead to new breakthroughs in cancer research.

It will be interesting to see if the recruitment of SH3BP4 by MC159 as a part of its anti-autophagy strategy is the only objective of this interaction or if SH3BP4 also serves other roles as a host cell factor exploited by MCV. In our preliminary studies, SH3BP4 binding capacity of MC159 showed no obvious correlation with transferrin receptor (TfR) turnover (C. Schmotz, unpublished data). However, given that SH3BP4 has been shown to regulate TfR internalization (37) and that extensive accumulation of TfR immunostaining has been reported in cells of molluscum bodies (4), this topic may need further experimental attention, as do the possible effects of MC159 on cell surface levels of others proteins involved in antiviral immunity.

In conclusion, we have shown that MC159 is a viral SH3 ligand that selectively chooses SH3BP4 as its cellular partner. This interaction strongly contributes to the capacity of MC159 to suppress cellular autophagy and may also have other effects on host cell physiology that remain to be characterized. Although no experimental models

exist for directly testing this assumption, it can be envisaged that SH3BP4 binding by MC159 helps MCV to escape from antiviral immunity to establish persistent infections. Current approaches to treat MCV lesions include topical application of immunostimulatory pharmaceuticals (1). The modest efficacy of such therapies could be greatly improved by developing approaches that would directly target the immunoevasion mechanisms of MCV. A more detailed understanding of host cell interactions of the multiple immunoregulatory molecules encoded by MCV, including hijacking of SH3BP4 by MC159, are needed to make this possible.

MATERIALS AND METHODS

Cell culture. Human embryonic kidney 293T (HEK293T), HeLa, and MCF7/LC3-EGFP cells were grown in Dulbecco's modified eagle medium (DMEM) (Sigma-Aldrich, St. Louis, MO, USA) supplemented with 4,500 mg/liter of glucose, 10% fetal bovine serum (FBS) (Gibco, Carlsbad, CA, USA), 0.05 mg/ml penicillin, 0.05 mg/ml streptomycin (Sigma-Aldrich), and 1 mM L-alanyl-L-glutamine (Sigma-Aldrich) at 37°C in 5% CO_2. For amino acid starvation to induce of autophagy in MCF7/LC3-EGFP cells, Hanks' balanced salt solution (HBSS) with $CaCl_2$ and $MgCl_2$ was used (Gibco, Carlsbad, CA, USA).

Plasmids. A synthetic fragment encoding the MC159L gene of molluscum contagiosum virus subtype 1 was purchased from GenScript (NJ, USA) and cloned into derivatives of the EF1-alpha promoter-driven mammalian expression vector pEBB (from Bruce Mayer, University of Connecticut [52]). The pEBB expression vectors contained either an N-terminal hemagglutinin (HA) tag or a transcarboxylase biotin acceptor domain (BD). For generation of the MC159 variants $MC159^{AXXA(N)}$, $MC159^{AXXA(C)}$, and $MC159^{AXXA(N+C)}$, all amino acid substitutions in MC159 were done by overlap PCR mutagenesis. An MC159(R197D) variant was generated by site-directed mutagenesis. The cDNA of human SH3BP4 (NCBI GeneID 23677) was inserted in the mammalian expression vector pCMV/myc-DEST via gateway cloning; pCMV/myc-DEST is a Myc epitope-containing derivate of the pCMV-DEST vector (35). The construction of an NF-κB-driven firefly luciferase expressing plasmid pBIIX has been described in Saksela and Baltimore (53). To create the pWPI-puro vector, we replaced EGFP in pWPI (from Didier Trono [plasmid 12254; Addgene]) with the puromycin resistance gene. For cell imaging studies, mCherry was fused to the C terminus of MC159 WT and the MC159-$^{AXXA(N)}$ variant, and the resulting constructs were subcloned into the constitutively expressing lentiviral plasmid pWPI-puro. Plasmid CAG-Cas9-T2A-EGFP-ires-puro was from Timo Otonkoski (plasmid 78311; Addgene). SH3BP4 genomic RNA (gRNA; BRDN0001487091) was a gift from John Doench and David Root (plasmid 78089; Addgene).

Antibodies and other reagents. The following antibodies were used: mouse anti-Myc (clone 9E10; Santa Cruz Biotechnology, TX, USA), mouse anti-SH3BP4 (A6; Santa Cruz Biotechnology), mouse anti-caspase-3 (BD Bioscience, CA, USA), mouse anti-caspase-8 (1C12; Cell Signaling Technology, MA, USA) rabbit anti-LC3B (D11) XP (Cell Signaling Technology, MA, USA), mouse monoclonal (6G6) to red fluorescent protein (RFP) (ChromoTek), rabbit anti-GFP (sc-8334; Santa Cruz Biotechnology), and rabbit anti-p62 (Enzo). IRDye 680CW goat anti-mouse IgG and IRDye 800CW goat anti-rabbit IgG were from Li-Cor Biotechnology.

Phage display. Ten-centimeter dishes of 293T cells were transfected with pEBB-BD-MC159 constructs or a control either by a standard calcium phosphate precipitation method (20 μg of plasmid DNA per dish) or by using polyethylenimine (PEI) (Polyscience, Inc., PA, USA). For the latter, 12 μg of plasmid DNA was mixed with PEI in Opti-MEM (Thermo Fisher Scientific, MA, USA) using a ratio of 1:2. At 48 h posttransfection, cells were collected in TEN (50 mM Tris [pH 7.4], 1 mM EDTA, 150 mM NaCl) buffer, pelleted at 4,000 rpm, and frozen for at least 15 min at −80°C. Subsequently, cells were thawed on ice and lysed in 1 ml of lysis buffer (phosphate-buffered saline [PBS], 1.2% [vol/vol] NP-40, protease inhibitor [Thermo Fisher Scientific, MA, USA]). The lysates were sonicated two times for 10 s each time at 50% amplitude and spun for 20 min at 13,200 rpm at 4°C. For precipitation of the BD fusion proteins, streptavidin-coated magnetic beads (Dynabeads M-280-Streptavidin; Invitrogen, CA, USA) were used according to the manufacturer's instructions. The pulldown was performed for 90 min at 4°C under rotation. Then the beads were washed once with 1 ml of cold lysis buffer and twice with 1 ml of cold PBST (PBS plus 0,05% Tween 20) for 1 min each wash.

For performing the SH3 phage display on the precipitated BD-fusion proteins, the target protein-containing beads were incubated with a mixture of human SH3 library-displaying phages about 1×10^{11} colony forming units (CFU) and 5% milk in PBST at a ratio of 2:1 for 90 min under rotation at room temperature. After incubation, beads were washed four times with 1 ml of 0.05% PBST for 5 min under rotation, and reaction tubes were changed after the first and third washes. Then the beads and bound phages were incubated with 800 μl of TG1 bacteria (optical density [OD] of 0.5 to 0.6) with shaking for 1 h at 37°C. Subsequently, bacteria were plated in different dilutions on ampicillin-containing lysogeny broth (LB) plates. Finally, individual colonies were sequenced for their SH3 domain-encoding phagemids (pG8J8/SH3 clones [34]) to identify the BD fusion protein SH3 interaction domains.

Cellular protein interactions. Cell culture and transfections were performed as described for the streptavidin pulldown of BD-tagged MC159. The ratio of the amount of transfected pEBB-BD-MC159 DNA to that of pCMV/DESTmyc-SH3BP4 DNA was 3:1. Frozen cell pellets were thawed on ice, lysed in 1 ml of lysis buffer (40 mM HEPES, 120 mM NaCl, 10 mM glycerophosphate, 1% [vol/vol] Triton X-100, protease, and phosphatase inhibitor minitablets [Thermo Fisher Scientific, MA, USA]), and incubated on ice for 20 min. After the lysates were cleared by centrifugation at 4°C, they were incubated with streptavidin-coated magnetic beads (Dynabeads M-280-Streptavidin; Invitrogen, CA, USA) for 90 min at 4°C under

rotation. Subsequently, the beads were washed three times with 1 ml of lysis buffer for 30 s and boiled in 4× Laemmli SDS-PAGE buffer. The precipitated proteins were separated and analyzed by standard Western blotting.

NF-κB luciferase reporter assay. 293T cells were seeded into 24-well plates and transfected with 50 ng of NF-κB-driven pBIIX-fLuc DNA, 50 ng of pEBB-HA-RenLuc, and 125 ng of pEBBHA-MC159 DNA using Fugene 6 (Promega, WI, USA) according to the manufacturer's instructions. At 24 h posttransfection, cells were treated with TNF-α-containing medium (10 ng/ml TNF-α) for 8 h. After treatment, cells were washed with PBS and lysed in 100 μl of passive lysis buffer (Promega, WI, USA). To assess luciferase activities, a dual-luciferase reporter assay system (Promega, WI, USA) was used according to the manufacturer's instructions. The measured *Renilla* luciferase was used as an internal control for each sample, and the values obtained for firefly luciferase were normalized according to levels in the measured controls.

TNF-induced apoptosis. Six-well plates of HeLa cells were transfected with either control plasmid DNA or pEBBHA-MC159 DNA using a previously described PEI transfection method. At 24 h posttransfection, cells were treated with medium containing 10 ng/ml TNF-α and 10 μg/ml cycloheximide for 8 h. After treatment, cells were washed once with PBS and lysed in 200 μl of NP-40 lysis buffer (150 mm NaCl, 50 mm Tris-HCl, pH 7.9, 1% Nonidet P-40). All samples were boiled in 4× Laemmli SDS-PAGE buffer, separated by SDS-PAGE, and analyzed for caspase-3 and -8 cleavage by Western blotting. Quantification of the signals obtained from Western blotting for full-length caspase-3 and cleaved caspase-8 was done using Image Studio Lite software (Li-Cor Biosciences).

SH3BP4 knockout cells. MCF7/LC3-EGFP cells were plated on six-well plates for 80% confluence after 24 h. Cells were cotransfected with 0.6 μg of Cas9 plasmid and 1.6 μg of SH3BP4 gRNA plasmid using TransIT-2020 (Mirus Bio) according to the manufacturer's instructions. At 48 h posttransfection, cells were selected with 4 μg/ml of puromycin for 2 days and then diluted in 96-well plates for single-cell selection.

Lentivirus-mediated gene transduction. pWPI-MC159-mCherry constructs were cotransfected with pDelta8.9 and vesicular stomatitis virus G protein (VSV-G) plasmids into HEK293T cells in complete medium using polyethylenimine. Supernatant was collected at 48 h posttransfection, filtered, and used to infect the wild-type or the SH3BP4 knockout MCF7/LC3-EGFP cells. Populations of infected cells stably transduced with wild-type or mutant MC159-mCherry were selected with puromycin.

Autophagy analyses. MCF7 cells expressing the macroautophagy marker LC3-EGFP alone or together with mCherry-fused wild-type MC159 or MC159$^{AXXA(N)}$ were plated on 13-mm-diameter number 1.5 coverslips. After 24 h the cells were washed twice with PBS and further cultured in complete medium (untreated) or in HBSS (starvation). After 6 h the cells were fixed with 4% paraformaldehyde (PFA) for 15 min, washed three times with PBS, and mounted with the nuclear marker Hoechst stain on microscope slides. Images were acquired on an Axio Imager Z2 upright microscope (Carl Zeiss Microscopy, GmbH, Germany) with a 20× (numeric aperture [NA],0.8) air immersion objective to a Hamamatsu Orca Flash 4.0 LT, 4-megapixel monochrome sCMOS camera. For each position three image stacks were acquired for the nuclear, EGFP, and mCherry channels. Image stacks were automatically deconvolved using the Huygens batch processing application (scientific volume imaging; Huygens Software). For each of the 12 experimental conditions (wild type, mutant, or no MC159/starvation or no treatment/parental MCF-7/LC3-EGFP cells or their SH3BP4 knockout derivatives), three independent, large experiments were carried out which involved two independent biological replicas for each condition. Quantitative autophagosome analysis was performed for the cells in several randomly picked areas from each biological replicate, amounting to a total of 20,181 parental and 12,538 SH3BP4 knockout cells examined for their autophagosome numbers. Statistical analysis to determine the significance of the differences in the observed autophagosome number variation was performed with a Mann-Whitney U test using IBM SPSS statistics software.

ACKNOWLEDGMENTS

We thank Virpi Syvälahti for expert technical assistance. This work used the services of the Biomedicum Imaging Unit and the Biostatistics Unit of the University of Helsinki.

This study was supported by grants to K.S. from the Academy of Finland (grant 259105), The Hospital District of Helsinki and Uusimaa (grant TYH2013406), and the Jane and Aatos Erkko Foundation (grant 160062). C.S. was supported in part by the Helsinki Graduate Program in Biotechnology and Molecular Biology.

REFERENCES

1. Chen X, Anstey AV, Bugert JJ. 2013. Molluscum contagiosum virus infection. Lancet Infect Dis 13:877–888. https://doi.org/10.1016/S1473-3099(13)70109-9.
2. Damon IK. 2013. Poxviruses, p 2160–2184. *In* Knipe DM, Howley PM, Cohen JI, Griffin DE, Lamb RA, Martin MA, Rancaniello VR, Roizman B (ed), Fields virology, 6 ed, vol 2. Lippincott Williams & Wilkins, Philadelphia, PA.
3. Gottlieb SL, Myskowski PL. 1994. Molluscum contagiosum. Int J Dermatol 33:453–461. https://doi.org/10.1111/j.1365-4362.1994.tb02853.x.
4. Viac J, Chardonnet Y. 1990. Immunocompetent cells and epithelial cell modifications in molluscum contagiosum. J Cutan Pathol 17:202–205. https://doi.org/10.1111/j.1600-0560.1990.tb00085.x.
5. Moss B, Shisler JL, Xiang Y, Senkevich TG. 2000. Immune-defense molecules of molluscum contagiosum virus, a human poxvirus. Trends Microbiol 8:473–477. https://doi.org/10.1016/S0966-842X(00)01838-2.
6. Senkevich TG, Koonin EV, Bugert JJ, Darai G, Moss B. 1997. The genome of molluscum contagiosum virus: analysis and comparison with other poxviruses. Virology 233:19–42. https://doi.org/10.1006/viro.1997.8607.

7. Bertin J, Armstrong RC, Ottilie S, Martin DA, Wang Y, Banks S, Wang GH, Senkevich TG, Alnemri ES, Moss B, Lenardo MJ, Tomaselli KJ, Cohen JI. 1997. Death effector domain-containing herpesvirus and poxvirus proteins inhibit both Fas- and TNFR1-induced apoptosis. Proc Natl Acad Sci U S A 94:1172–1176. https://doi.org/10.1073/pnas.94.4.1172.
8. Hu S, Vincenz C, Buller M, Dixit VM. 1997. A novel family of viral death effector domain-containing molecules that inhibit both CD-95- and tumor necrosis factor receptor-1-induced apoptosis. J Biol Chem 272:9621–9624. https://doi.org/10.1074/jbc.272.15.9621.
9. Thome M, Schneider P, Hofmann K, Fickenscher H, Meinl E, Neipel F, Mattmann C, Burns K, Bodmer JL, Schroter M, Scaffidi C, Krammer PH, Peter ME, Tschopp J. 1997. Viral FLICE-inhibitory proteins (FLIPs) prevent apoptosis induced by death receptors. Nature 386:517–521. https://doi.org/10.1038/386517a0.
10. Irmler M, Thome M, Hahne M, Schneider P, Hofmann K, Steiner V, Bodmer JL, Schroter M, Burns K, Mattmann C, Rimoldi D, French LE, Tschopp J. 1997. Inhibition of death receptor signals by cellular FLIP. Nature 388:190–195. https://doi.org/10.1038/40657.
11. Safa AR. 2012. c-FLIP, a master anti-apoptotic regulator. Exp Oncol 34:176–184.
12. Shisler JL. 2015. Immune evasion strategies of molluscum contagiosum virus. Adv Virus Res 92:201–252. https://doi.org/10.1016/bs.aivir.2014.11.004.
13. Fu TM, Li Y, Lu A, Li Z, Vajjhala PR, Cruz AC, Srivastava DB, DiMaio F, Penczek PA, Siegel RM, Stacey KJ, Egelman EH, Wu H. 2016. Cryo-EM structure of caspase-8 tandem DED filament reveals assembly and regulation mechanisms of the death-inducing signaling complex. Mol Cell 64:236–250. https://doi.org/10.1016/j.molcel.2016.09.009.
14. Thurau M, Everett H, Tapernoux M, Tschopp J, Thome M. 2006. The TRAF3-binding site of human molluscipox virus FLIP molecule MC159 is critical for its capacity to inhibit Fas-induced apoptosis. Cell Death Differ 13:1577–1585. https://doi.org/10.1038/sj.cdd.4401847.
15. Guasparri I, Keller SA, Cesarman E. 2004. KSHV vFLIP is essential for the survival of infected lymphoma cells. J Exp Med 199:993–1003. https://doi.org/10.1084/jem.20031467.
16. Sun Q, Matta H, Chaudhary PM. 2003. The human herpes virus 8-encoded viral FLICE inhibitory protein protects against growth factor withdrawal-induced apoptosis via NF-kappa B activation. Blood 101:1956–1961. https://doi.org/10.1182/blood-2002-07-2072.
17. Biswas S, Shisler JL. 2017. Molluscum contagiosum virus MC159 abrogates cIAP1-NEMO interactions and inhibits NEMO polyubiquitination. J Virol 91:e00276-17. https://doi.org/10.1128/JVI.00276-17.
18. Randall CM, Jokela JA, Shisler JL. 2012. The MC159 protein from the molluscum contagiosum poxvirus inhibits NF-kappaB activation by interacting with the IκB kinase complex. J Immunol 188:2371–2379. https://doi.org/10.4049/jimmunol.1100136.
19. Randall CM, Biswas S, Selen CV, Shisler JL. 2014. Inhibition of interferon gene activation by death-effector domain-containing proteins from the molluscum contagiosum virus. Proc Natl Acad Sci U S A 111:E265–E272. https://doi.org/10.1073/pnas.1314569111.
20. Lee JS, Li Q, Lee JY, Lee SH, Jeong JH, Lee HR, Chang H, Zhou FC, Gao SJ, Liang C, Jung JU. 2009. FLIP-mediated autophagy regulation in cell death control. Nat Cell Biol 11:1355–1362. https://doi.org/10.1038/ncb1980.
21. Choi Y, Bowman JW, Jung JU. 2018. Autophagy during viral infection—a double-edged sword. Nat Rev Microbiol 16:341–354. https://doi.org/10.1038/s41579-018-0003-6.
22. Dong X, Levine B. 2013. Autophagy and viruses: adversaries or allies? J Innate Immun 5:480–493. https://doi.org/10.1159/000346388.
23. Jordan TX, Randall G. 2012. Manipulation or capitulation: virus interactions with autophagy. Microbes Infect 14:126–139. https://doi.org/10.1016/j.micinf.2011.09.007.
24. Davey NE, Trave G, Gibson TJ. 2011. How viruses hijack cell regulation. Trends Biochem Sci 36:159–169. https://doi.org/10.1016/j.tibs.2010.10.002.
25. Mayer BJ. 2015. The discovery of modular binding domains: building blocks of cell signalling. Nat Rev Mol Cell Biol 16:691–698. https://doi.org/10.1038/nrm4068.
26. Saksela K, Permi P. 2012. SH3 domain ligand binding: What's the consensus and where's the specificity? FEBS Lett 586:2609–2614. https://doi.org/10.1016/j.febslet.2012.04.042.
27. Hiipakka M, Poikonen K, Saksela K. 1999. SH3 domains with high affinity and engineered ligand specificities targeted to HIV-1 Nef. J Mol Biol 293:1097–1106. https://doi.org/10.1006/jmbi.1999.3225.
28. Lee CH, Saksela K, Mirza UA, Chait BT, Kuriyan J. 1996. Crystal structure of the conserved core of HIV-1 Nef complexed with a Src family SH3 domain. Cell 85:931–942. https://doi.org/10.1016/S0092-8674(00)81276-3.
29. Saksela K, Cheng G, Baltimore D. 1995. Proline-rich (PxxP) motifs in HIV-1 Nef bind to SH3 domains of a subset of Src kinases and are required for the enhanced growth of Nef$^+$ viruses but not for down-regulation of CD4. EMBO J 14:484–491. https://doi.org/10.1002/j.1460-2075.1995.tb07024.x.
30. Amako Y, Igloi Z, Mankouri J, Kazlauskas A, Saksela K, Dallas M, Peers C, Harris M. 2013. Hepatitis C virus NS5A inhibits mixed lineage kinase 3 to block apoptosis. J Biol Chem 288:24753–24763. https://doi.org/10.1074/jbc.M113.491985.
31. Fackler OT, Wolf D, Weber HO, Laffert B, D'Aloja P, Schuler-Thurner B, Geffin R, Saksela K, Geyer M, Peterlin BM, Schuler G, Baur AS. 2001. A natural variability in the proline-rich motif of Nef modulates HIV-1 replication in primary T cells. Curr Biol 11:1294–1299. https://doi.org/10.1016/S0960-9822(01)00373-6.
32. Heikkinen LS, Kazlauskas A, Melen K, Wagner R, Ziegler T, Julkunen I, Saksela K. 2008. Avian and 1918 Spanish influenza a virus NS1 proteins bind to Crk/CrkL Src homology 3 domains to activate host cell signaling. J Biol Chem 283:5719–5727. https://doi.org/10.1074/jbc.M707195200.
33. Neuvonen M, Kazlauskas A, Martikainen M, Hinkkanen A, Ahola T, Saksela K. 2011. SH3 domain-mediated recruitment of host cell amphiphysins by alphavirus nsP3 promotes viral RNA replication. PLoS Pathog 7:e1002383. https://doi.org/10.1371/journal.ppat.1002383.
34. Kärkkäinen S, Hiipakka M, Wang JH, Kleino I, Vähä-Jaakkola M, Renkema GH, Liss M, Wagner R, Saksela K. 2006. Identification of preferred protein interactions by phage-display of the human Src homology-3 proteome. EMBO Rep 7:186–191. https://doi.org/10.1038/sj.embor.7400596.
35. Kazlauskas A, Schmotz C, Kesti T, Hepojoki J, Kleino I, Kaneko T, Li SS, Saksela K. 2016. Large-scale screening of preferred interactions of human Src homology-3 (SH3) domains using native target proteins as affinity ligands. Mol Cell Proteomics 15:3270–3281. https://doi.org/10.1074/mcp.M116.060483.
36. Dunlevy JR, Berryhill BL, Vergnes JP, SundarRaj N, Hassell JR. 1999. Cloning, chromosomal localization, and characterization of cDNA from a novel gene, SH3BP4, expressed by human corneal fibroblasts. Genomics 62:519–524. https://doi.org/10.1006/geno.1999.5994.
37. Tosoni D, Puri C, Confalonieri S, Salcini AE, De Camilli P, Tacchetti C, Di Fiore PP. 2005. TTP specifically regulates the internalization of the transferrin receptor. Cell 123:875–888. https://doi.org/10.1016/j.cell.2005.10.021.
38. Gil J, Rullas J, Alcami J, Esteban M. 2001. MC159L protein from the poxvirus molluscum contagiosum virus inhibits NF-kappaB activation and apoptosis induced by PKR. J Gen Virol 82:3027–3034. https://doi.org/10.1099/0022-1317-82-12-3027.
39. Murao LE, Shisler JL. 2005. The MCV MC159 protein inhibits late, but not early, events of TNF-alpha-induced NF-κB activation. Virology 340:255–264. https://doi.org/10.1016/j.virol.2005.06.036.
40. Shisler JL, Moss B. 2001. Molluscum contagiosum virus inhibitors of apoptosis: The MC159 v-FLIP protein blocks Fas-induced activation of procaspases and degradation of the related MC160 protein. Virology 282:14–25. https://doi.org/10.1006/viro.2001.0834.
41. Garvey T, Bertin J, Siegel R, Lenardo M, Cohen J. 2002. The death effector domains (DEDs) of the molluscum contagiosum virus MC159 v-FLIP protein are not functionally interchangeable with each other or with the DEDs of caspase-8. Virology 300:217–225. https://doi.org/10.1006/viro.2002.1518.
42. Kim YM, Kim DH. 2013. dRAGging amino acid-mTORC1 signaling by SH3BP4. Mol Cells 35:1–6. https://doi.org/10.1007/s10059-013-2249-1.
43. Kim YM, Stone M, Hwang TH, Kim YG, Dunlevy JR, Griffin TJ, Kim DH. 2012. SH3BP4 is a negative regulator of amino acid-Rag GTPase-mTORC1 signaling. Mol Cell 46:833–846. https://doi.org/10.1016/j.molcel.2012.04.007.
44. Høyer-Hansen M, Bastholm L, Szyniarowski P, Campanella M, Szabadkai G, Farkas T, Bianchi K, Fehrenbacher N, Elling F, Rizzuto R, Mathiasen IS, Jäättelä M. 2007. Control of macroautophagy by calcium, calmodulin-dependent kinase kinase-beta, and Bcl-2. Mol Cell 25:193–205. https://doi.org/10.1016/j.molcel.2006.12.009.
45. Kim E, Goraksha-Hicks P, Li L, Neufeld TP, Guan KL. 2008. Regulation of TORC1 by Rag GTPases in nutrient response. Nat Cell Biol 10:935–945. https://doi.org/10.1038/ncb1753.
46. Kim J, Kim E. 2016. Rag GTPase in amino acid signaling. Amino Acids 48:915–928. https://doi.org/10.1007/s00726-016-2171-x.

47. Klionsky DJ, Abdelmohsen K, Abe A, Abedin MJ, Abeliovich H, Acevedo Arozena A, Adachi H, Adams CM, Adams PD, Adeli K, Adhihetty PJ, Adler SG, Agam G, Agarwal R, Aghi MK, Agnello M, Agostinis P, Aguilar PV, Aguirre-Ghiso J, Airoldi EM, Ait-Si-Ali S, Akematsu T, Akporiaye ET, Al-Rubeai M, Albaiceta GM, Albanese C, Albani D, Albert ML, Aldudo J, Algül H, Alirezaei M, Alloza I, Almasan A, Almonte-Beceril M, Alnemri ES, Alonso C, Altan-Bonnet N, Altieri DC, Alvarez S, Alvarez-Erviti L, Alves S, Amadoro G, Amano A, Amantini C, Ambrosio S, Amelio I, Amer AO, Amessou M, Amon A, An Z, et al. 2016. Guidelines for the use and interpretation of assays for monitoring autophagy (3rd edition). Autophagy 12:1–222. https://doi.org/10.1080/15548627.2015.1100356.
48. Komatsu M, Waguri S, Koike M, Sou YS, Ueno T, Hara T, Mizushima N, Iwata J, Ezaki J, Murata S, Hamazaki J, Nishito Y, Iemura S, Natsume T, Yanagawa T, Uwayama J, Warabi E, Yoshida H, Ishii T, Kobayashi A, Yamamoto M, Yue Z, Uchiyama Y, Kominami E, Tanaka K. 2007. Homeostatic levels of p62 control cytoplasmic inclusion body formation in autophagy-deficient mice. Cell 131:1149–1163. https://doi.org/10.1016/j.cell.2007.10.035.
49. Stein U, Walther W, Arlt F, Schwabe H, Smith J, Fichtner I, Birchmeier W, Schlag PM. 2009. MACC1, a newly identified key regulator of HGF-MET signaling, predicts colon cancer metastasis. Nat Med 15:59–67. https://doi.org/10.1038/nm.1889.
50. Wilkins OM, Titus AJ, Salas LA, Gui J, Eliot M, Butler RA, Sturgis EM, Li G, Kelsey KT, Christensen BC. 2019. MicroRNA-related genetic variants associated with overall survival of head and neck squamous cell carcinoma. Cancer Epidemiol Biomarkers Prev 28:127–136. https://doi.org/10.1158/1055-9965.Epi-18-0002.
51. Zhang X, Yao X, Qin C, Luo P, Zhang J. 2016. Investigation of the molecular mechanisms underlying metastasis in prostate cancer by gene expression profiling. Exp Ther Med 12:925–932. https://doi.org/10.3892/etm.2016.3376.
52. Tanaka M, Gupta R, Mayer BJ. 1995. Differential inhibition of signaling pathways by dominant-negative SH2/SH3 adapter proteins. Mol Cell Biol 15:6829–6837. https://doi.org/10.1128/MCB.15.12.6829.
53. Saksela K, Baltimore D. 1993. Negative regulation of immunoglobulin kappa light-chain gene transcription by a short sequence homologous to the murine B1 repetitive element. Mol Cell Biol 13:3698–3705. https://doi.org/10.1128/MCB.13.6.3698.